REGISTRATION OF TEXTURED REMOTE SENSING IMAGES USING DIRECTIONAL GABOR FRAMES

Hannah Olson [1], *Wojciech Czaja* [1], *and Jacqueline Le Moigne* [2]

[1]Mathematics Department, University of Maryland, College Park, MD, 20742, USA

[2] Software Engineering Division, NASA Goddard Space Flight Center, Greenbelt, MD, 20771, USA

ABSTRACT

In this paper we propose to utilize a new concept of discrete directional Gabor frames for automatic image registration. The directional Gabor representations have been shown to provide more accurate feature extraction than directional wavelet transforms for images where texture is the dominant feature. Initial experimental results are presented here which indicate that discrete directional Gabor frames exhibit strong correlations, which indicates that they are likely to improve the existing image registration toolbox.

Index Terms-- Image registration, Gabor systems, Remotely-sensed

1. INTRODUCTION

A major challenge to the field of remote sensing is to create an accurate and robust system for automatic image registration. The goal of image registration is to align two images that represent the same scene but taken under different conditions. This is done by treating one image, known as the reference, as static and then finding a transformation for the second image, known as the input, that will align it with the reference [1].

Methods based on wavelets and shearlets have been shown to be effective for registration of most remotely-sensed images [1], [2]. However, these methods do not perform particularly well on images where texture is the dominant feature, or for multisensor image registration such as LIDAR-to- optical registration [1].

Recently, discrete directional Gabor frames have been shown to be better at representing images where texture is the dominant feature [3]. This method of representation captures information about not only textural features within an image, but also their direction. In this paper, we provide evidence that the discrete directional Gabor frames will be able to perform well for automated registration of remotely-sensed images where texture is the dominant feature.

2. BACKGROUND ON AUTOMATED IMAGE REGISTRATION

As was previously defined, image registration is the process by which two images, or one image and a map, get aligned. In the remote sensing domain, we can assume that a prior alignment has been performed using navigation input, i.e., through what is called "systematic correction". Image registration is the "precision correction" step, which is feature-based, i.e., based on information included in the images. Any image registration algorithm can be described by three main components: (1) feature extraction, (2) similarity metrics, and (3) feature matching. In this work, we mainly concentrate on the feature extraction component. Our team previously performed extensive work with automated image registration algorithms based on features extracted from wavelet and shearlet decompositions. In [2], we looked at orthonormal (e.g., Daubechies') and Spline wavelet decompositions, as well as at the wavelet-like Simoncelli overcomplete representation. When compared using an L2 Norm and a Levenberg-Marquart optimization, results showed that Spline and Simoncelli features perform better than orthonormal wavelets, that Simoncelli features offered a better performance in terms of accuracy, but that Spline wavelet features are more robust when the initial conditions are further from the optimal solution. In [1], with the goal of improving the robustness of this image registration algorithm to the initial conditions, we then investigated the use of shearlets as compared to wavelets and to Simoncelli; this study showed that shearlet features are more robust to the initial conditions than wavelet or Simoncelli features but, when close to the solution, Simoncelli still get the best accuracy. A combination of shearlets and Simoncelli features was then proposed and outperformed all other features for both accuracy and performance. The remaining challenge came with textured images, in particular LIDAR images of forested areas which did not present well contrasted features, and for which no specific feature extraction methods, included edge detection, SIFT detector, or wavelet/shearlet decompositions provided

satisfactory results. This led us to investigate the use of the directional Fourier transform.

3. DIRECTIONAL FOURIER TRANSFORM

Counter to a common belief in image analysis that wavelet-based techniques are superior to other approaches, Fourier and Gabor methods play a significant role, see, eg, [4, 5, 6, 7]. In this regard, Grafakos and Sansing proposed the concept of directional time-frequency analysis in [8]. They introduce directional sensitivity in the time-frequency setting by considering projections onto the elements of the unit sphere. The Radon transform arises naturally in this context and it enables continuous and semi-continuous reconstruction formulas.

Czaja et al [3] developed a theory of discrete directional Gabor frames, related to the concept of Gabor ridge systems of Grafakos and Sansing. They considered elements of the form:

$g_{m,t,u}(x) := g^{m,t}(u \cdot x), m, t \in \mathbb{R},\ u \in S^{d-1}, x \in \mathbb{R}^d$

for a given function $g : \mathbb{R} \to \mathbb{C}$. The construction results in a discrete frame:

$$\{g_{m,t,u}\}_{(m,t,u)\in\Lambda},$$

Such a system is called a *discrete directional Gabor frame*.

A natural choice for the window function is $g(x) = sinc(\frac{x}{16})^4$, due to its compact Fourier support $K = [-\frac{1}{4}, \frac{1}{4}]$. The indexing set,

$\Lambda \subset \Lambda_\omega = \{(m, n, u) \mid ((u, m) \subset \mathbb{S}^1 \times \mathbb{R}\ , n \in \omega\mathbb{Z}\} \subset \mathbb{R} \times \mathbb{R} \times S^{d-1}$

must be discrete with respect to the natural topology of $\mathbb{R} \times \mathbb{R} \times S^{d-1}$. We chose its bounded finite subset so that for a 2M X 2N image $A = ([-M, M-1] \times [-N, N]) \cap \mathbb{Z}^2, u \in \left\{\frac{(x_1,x_2)}{\|(x_1,x_2)\|_2} \ :\ (x_1, x_2) \in A,\ \gcd(x_1, x_2) = 1\right\}$. The translation parameter runs over the set n = 4k, |k| ≤ 5 for integers k.

4. METHODS

Experiments were performed on a real image that was synthetically transformed. The image was based on a 1024 x 1024 image extracted from Band 4 of a Landsat-TM scene of the Mount Hood National Forest. The reference image and each input image were run through the code for discrete directional Gabor frames and the *dual*, the vector of coefficients, was extracted.

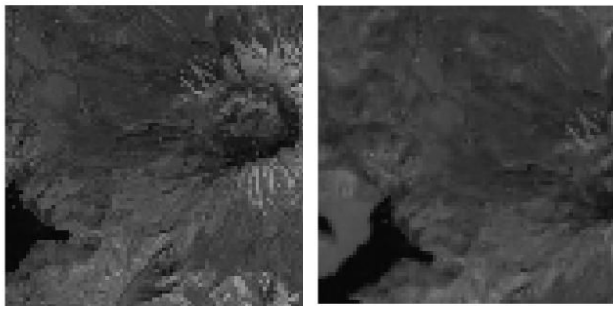

Fig. 1 Reference image (left) and input image, which has been translated -10 pixels in the x-direction and rotated 10 degrees clockwise (right)

Then, the mean square error (MSE) between the dual of the reference image and the input image was taken. The equation for MSE is given by,

$$MSE = \sum_{i=1}^{N} \sqrt{(D_R(i) - D_{I0(i)})^2} \quad (1)$$

where N is the length of the dual vectors. The MSE was used as a similarity metric between pairs of image duals.

To generate the reference image, shown on the left of Figure 1, an 85 x 85 sub-image was extracted from the Mount Hood image. To generate the first input image, the entire Mount Hood image was rotated 10 degrees clockwise. From this rotated image, a 85 x 85 sub-image was extracted 10 pixels to the left of the center of the rotated image, as shown on the right on Figure 1. This off-center extraction was used as a proxy for a translation of -10 pixels in the x-direction. The discrete directional Gabor frame transform was then performed on both the input image and the reference image. Using (1), the MSE between the two dual vectors was calculated. 881 total reference images were generated each with an integer rotation angle between -10 degrees counter-clockwise and 10 degrees counter-clockwise and either an integer translation between -10 pixels and 10 pixels in the x-direction and 0 pixels in the y-direction, or an integer translation between -10 pixels and 10 pixels in the y-direction and 0 pixels in the x-direction. The MSE was calculated between the dual for the reference image and the dual for each of the input images. Finally, the MSEs were averaged between the cases with no translation in the x-direction and the cases with no translation in the y-direction and the results are shown in Figure 2.

To see what effect noise had on the results, the experiments were repeated with white Gaussian noise

randomly added to each of the input images before running through the discrete directional Gabor frame transform.

5. RESULTS

At each of the three levels of noise, the MSE is smallest where the transformation is smallest and it grows as the transformation grows. However, the error does not grow uniformly. Figure 2 shows that small changes in rotation angle with no translation produce a much larger MSE than small translations with no rotation angle. This can be explained by the fact that the discrete directional Gabor frames contain directional information, which will naturally change as the rotation angle changes, but will not necessarily change for small translations.

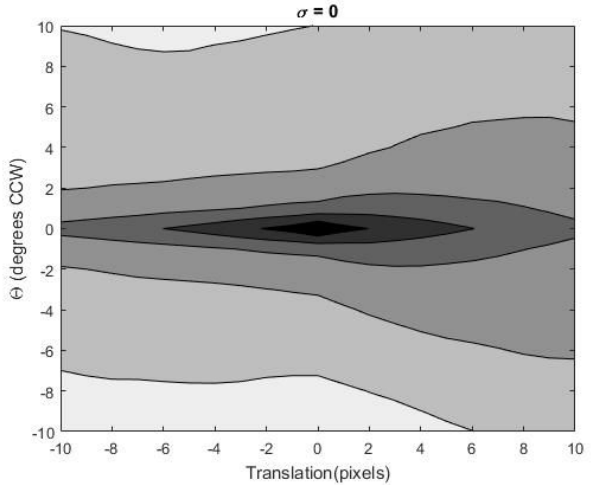

Fig. 2 Results from no added noise

Figures 2, 3, and 4 show MSE as a function of translation, in pixels, and rotation angle, in degrees counter-clockwise. The MSE is shaded in steps of 75, with black representing transformations that produced an MSE of less than 75.

At small levels of noise, the results still show a fairly strong correlation. As σ increases linearly, the MSE grows exponentially. Above a value of -35, the correlation between the reference and the dual is weak and likely would be unable to successfully be registered. Figure 4 shows a large area where all of the MSEs are between 300 and 375 (the darkest region in Figure 4).

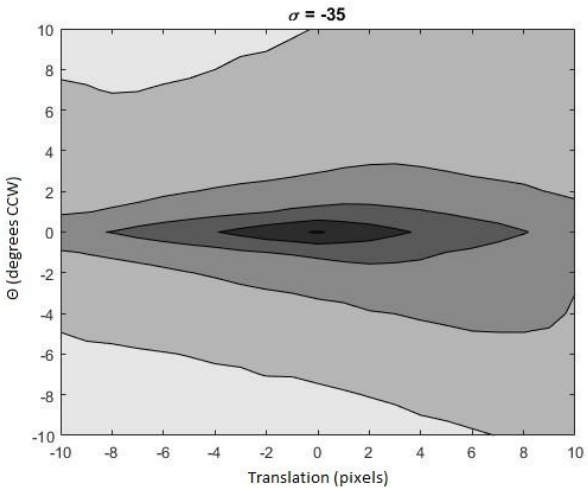

Fig. 3 Results from noise with σ=-35

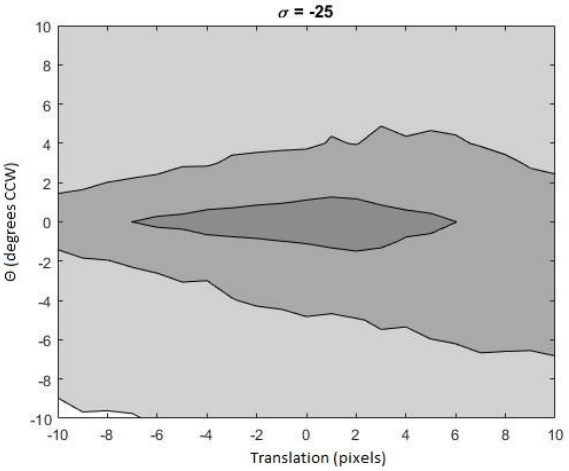

Fig. 4 Results from noise with σ = -25

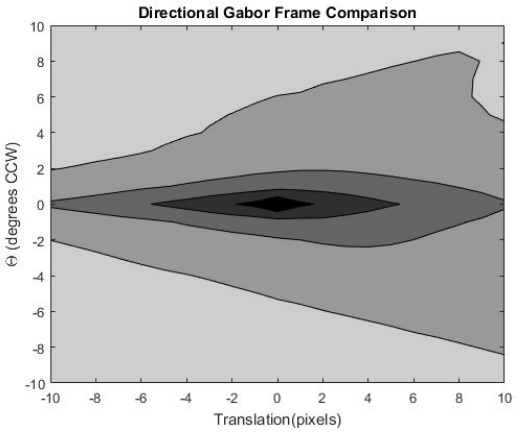

Fig. 5 Normalized results from the discrete directional Gabor frames. This is the data from Figure 2 normalized.

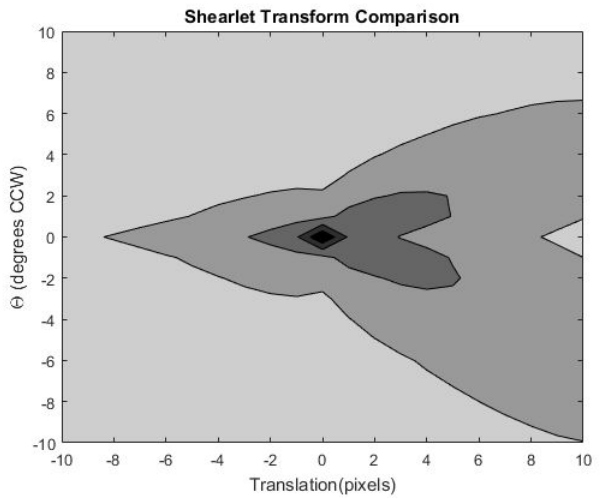

Fig. 6 Normalized shearlet transform comparison

6. CONCLUSION

The results presented in this paper show a good indication that discrete directional Gabor frames can be successfully used to perform automatic image registration. When comparing Directional Gabor to Shearlets [1], we can see from the 2 plots shown in Figures 5 and 6 that the Directional Gabor results show lower errors for larger values of rotation and translation than the Shearlet results. This indicates that Directional Gabor features should be more reliable to larger transformations than Shearlets. Additional experimental results will be shown at the conference. In the future, experiments should be conducted using one or more different images with synthetic transformations, and on multi-sensor images.

7. ACKNOWLEDGEMENTS

This work was supported in part by a research grant from NASA, NNX17AJ11G" A Dinurnal Constellation of Miniaturized Imaging Spectrometers for Vegetation Structure and Funtion - MiniSpec" and the NASA Office of Education OSSI student internship program.

8. REFERENCES

[1] J.M. Murphy, J. Le Moigne, and D.J. Harding. "Automatic Image Registration of Multimodal Remotely Sensed Data With Global Shearlet Features." *IEEE Transactions on Geoscience and Remote Sensing* 54, no. 3 (03 2016): 1685-704.

[2] I. Zavorin, and J. Le Moigne. "Use of Multiresolution Wavelet Feature Pyramids for Automatic Registration of Multisensor Imagery." *IEEE Transactions on Image Processing* 14, no. 6 (06 2005): 770-82.

[3] W. Czaja, B. Manning, J. Murphy, and K. Stubbs. Gabor frames and directional time-frequency analysis. Applied and Computational Harmonic Analysis, In Press, 2017.

[4] M. Porat and Y. Y. Zeevi. Localized texture processing in vision: analysis and synthesis in gaborian space. IEEE Transactions on Biomedical Engineering, 36:115–129, 1989.

[5] Y. Shi, X. Yang, and Y. Guo. Translation invariant directional framelet transform combined with Gabor filters for image denoising. Image Processing, IEEE Transactions on, 23:44–55, 2014.

[6] W. Czaja and M.V. Wickerhauser. Singularity detection in images using dual local autocovariance. Applied and Computational Harmonic Analysis, 13(1):77–88, 2002.

[7] M.V. Wickerhauser and W. Czaja. A simple nonlinear filter for edge detection in images. Proc. SPIE, 5439, 2004.

[8] L. Grafakos and C. Sansing. Gabor frames and directional time-frequency analysis. Applied and Computational Harmonic Analysis, 25(1):47–67, 2008.